Cancer Letters 371 (2016) 143–150

Contents lists available at ScienceDirect

Cancer Letters

journal homepage: www.elsevier.com/locate/canlet

Original Articles

Hypoxia but not normoxia promotes Smoothened transcription through upregulation of RBPJ and Mastermind-like 3 in pancreatic cancer

Hideya Onishi [a,*], Akio Yamasaki [a], Makoto Kawamoto [a], Akira Imaizumi [a,b], Mitsuo Katano [a]

[a] Department of Cancer Therapy and Research, Graduate School of Medical Sciences, Kyushu University, Fukuoka, Japan
[b] Shukoukai Inc., Tokyo, Japan

ARTICLE INFO

Article history:
Received 17 August 2015
Received in revised form 5 November 2015
Accepted 5 November 2015

Keywords:
Hypoxia
Hedgehog signaling
Smoothened
Mastermind-like 3
RBPJ
Pancreatic cancer

ABSTRACT

We previously demonstrated that Hedgehog (Hh) signaling is activated under hypoxia through upregulation of transcription of Smoothened (SMO) gene. However, the mechanism of hypoxia-induced activation of SMO transcription remains unclear. In the analysis of altered expressions of genes related to Hh signaling between under normoxia and hypoxia by DNA microarray analysis, we picked up 2 genes, a transcriptional regulator, recombination signal binding protein for immunoglobulin-kappa-J region (RBPJ) and a transcriptional co-activator, Mastermind-like 3 (MAML3). Expressions of SMO, MAML3 and RBPJ were increased under hypoxia in pancreatic ductal adenocarcinoma cells (PDAC). RBPJ and MAML3 inhibition under hypoxia led to decreased SMO and GLI1 expressions, whereas SMO expression in MAML3-inhibited and RBPJ-inhibited cells under normoxia showed no change. However, overexpression of RBPJ under normoxia led to increased SMO expression. Additionally, cells knocked down for MAML3 and RBPJ inhibition under hypoxia showed decreased invasiveness through matrix metalloproteinase-2 suppression and decreased proliferation. Xenograft mouse models showed that MAML3 and RBPJ knockdown inhibited tumorigenicity and tumor volume. Our results suggest that hypoxia promotes SMO transcription through upregulation of MAML3 and RBPJ to induce proliferation, invasiveness and tumorigenesis in pancreatic cancer.

© 2015 Elsevier Ireland Ltd. All rights reserved.

Introduction

In vivo environment, especially tumor local site locates under hypoxic condition [1,2]. The oxygen tension in tumor local sites is <1.3% O_2, compared with 5.3% in mixed venous blood and 3.3–7.9% in well-vascularized organs [2,3]. Accordingly, much research has been focused on elucidating the mechanisms and pathways underlying hypoxic conditions. We previously demonstrated that Hedgehog (Hh) signaling is activated under hypoxic condition through upregulation of transcription of Smoothened (SMO), a key protein that drives Hh signaling [4]. Furthermore, we showed that Hh signaling activation by hypoxia leads to the induction of malignant phenotypes, such as proliferation and invasiveness, in pancreatic cancer [4,5]. Consistent with our results, Lei et al. recently revealed that hypoxia induces epithelial to mesenchymal transition through hypoxia-related SMO upregulation, Hh signaling activation [6]. Moreover, Spivak-Kroizman et al. have shown that hypoxia triggers Hh-mediated tumor–stromal interactions in pancreatic cancer [7]. However, the mechanism of hypoxia-induced activation of SMO transcription remains unclear.

Currently, many Hh signaling inhibitors are under clinical study [8–10] and the US Food and Drug Administration recently approved a SMO inhibitor, vismodegib, for the treatment of metastatic or unresectable basal cell carcinomas of the skin [11]. However, promising results in pancreatic cancer treatment have not yet been reported. To develop a more effective therapeutic strategy against pancreatic cancer using Hh signaling inhibitors, understanding the mechanism underlying hypoxia-induced upregulation of SMO transcription is critical.

In the present study, we aimed to clarify the mechanism underlying altered transcription of SMO under hypoxic conditions to help contribute to the development of new effective therapeutic strategies for refractory pancreatic cancer by improving the effects of Hh signaling inhibitors.

Materials and methods

Cell culture and reagents

Two human pancreatic ductal adenocarcinoma cells (PDAC) lines (ASPC-1 and SUIT-2) were maintained in RPMI 1640 medium (Nacalai Tesque, Kyoto, Japan)

* Corresponding author. Tel.: +81 92 642 6220; fax: +81 92 642 6221.
E-mail address: ohnishi@surg1.med.kyushu-u.ac.jp (H. Onishi).

http://dx.doi.org/10.1016/j.canlet.2015.11.012
0304-3835/© 2015 Elsevier Ireland Ltd. All rights reserved.

supplemented with 10% fetal calf serum (FCS; Life Technologies, Grand Island, NY) and antibiotics (100 units/ml of penicillin and 100 μg/ml of streptomycin). For normoxic conditions, cells were cultured in 5% CO_2 and 95% air. For hypoxic conditions, cells were cultured in 1% O_2, 5% CO_2, and 94% N_2 using a multigas incubator (Sanyo, Tokyo, Japan). PDAC cultured under normoxia or hypoxia for 24 h were used for experimental analyses as described below.

Cell proliferation assay

PDAC (1×10^5 cells/well) were plated to 6-well plates and were cultured under hypoxia for 3 days. Cell numbers were counted by light microscopy every day. The experiments were performed in triplicate wells.

DNA microarray

The cRNA was amplified, labeled, and hybridized according to the recommended protocol from Agilent. Relative hybridization intensities and background hybridization values were calculated using Agilent Feature Extraction Software. We calculated Z-scores and ratios from the normalized signal intensities of each probe for comparison between ASPC-1 cells cultured under hypoxia for 2 days and ASPC-1 cells continuously cultured under normoxia. We selected genes that were related to Hh signaling that showed a change in expression of ≥2.0-fold.

Real-time PCR

Total RNA was extracted using the High Pure RNA Isolation Kit (Roche, Mannheim, Germany) and quantified by spectrophotometry (Ultrospec 2100 Pro; Amersham Pharmacia Biotech, Cambridge, United Kingdom). For real-time RT-PCR, 1 μg of RNA was treated with DNase and reverse transcribed to cDNA with the Quantitect Reverse Transcription Kit (Qiagen, Valencia, CA, USA) according to the manufacturer's protocol. Reactions were run with iQ™ SYBR Green Supermix (Bio-Rad) on a DNA Engine Option 2 System (MJ Research, Waltham, MA). All primer sets amplified fragments less than 200 bp long. The primer sequences used were as follows: *SMO*, forward, CAGGTGGATGGGGACTCTGTGAGT, reverse, GAGTCATGACTCCTCGGATGAGG; *MAML3*, forward, 5′-AAGCCCAGGGACCGAGGCAA-3′, reverse, 5′-GCAGCCTTGGAGGGGCTTGG-3′; *GLI1*, forward, 5′-GGTTCAAGAGCCTGGGCTGTGT-3′, reverse, 5′-GGCAGCATTCTC AGTGATGCTG-3′; *RBPJ*, forward, 5′-CGCA TTATTGGATGCAGATG-3′, reverse, 5′-CAGGAAGCGCCATCATTTAT-3′; *matrix metalloproteinase (MMP-9)*, forward, 5′-TGGGCTACGTGACCTATGACAT-3′, reverse, 5′-GCCCAGCCCACCTCCACTCCTC-3′; *MMP-2*, forward, 5′-TGATCTTGACCAGAATACCA TCGA-3′, reverse, 5′-GGCTTGCGA GGGAAGAAGTT-3′; and *β-actin*, forward, 5′-TTGCCGACAGGATGCAGAAGGA-3′, and reverse, 5′-AGGTGGACAGCGAGGCCAGGAT-3′. The amount of each target gene in a given sample was normalized to the level of *β-actin*.

Matrigel invasion assay

Cell invasion assays were performed using Matrigel-coated transwell inserts as described previously [12]. In brief, the upper surface of a filter (pore size, 8.0 μm; BD Biosciences, Heidelberg, Germany) was coated with Matrigel basement membrane (BD Biosciences). Cells were suspended in RPMI-1640 with 10% FCS. Next we added 0.8×10^5 cells to the upper chamber and incubated the cells for 16 h under hypoxia. After incubation, the filter was fixed and stained with Diff-Quick reagent (International Reagents, Kobe, Japan). All cells that had migrated from the upper to the lower side of the filter were counted under a light microscope (BX50; Olympus, Tokyo, Japan) at a magnification of ×100. Tumor cell invasiveness was performed in triplicate wells.

RNA interference

Small interfering RNA (siRNA) for *MAML3* (ON-TARGET *plus* SMART pool, L-013813), siRNA for *HIF-1α* (ON-TARGET *plus* SMART pool, L-004018), siRNA for *RBPJ* (ON-TARGET *plus* SMART pool, L-007772) and negative control siRNA (ON-TARGET *plus* si CONTROL non-targeting pool, D-001810) were purchased from Dharmacon RNA Technologies (Chicago, IL). Cells (0.2×10^6 cells/well) seeded in 6-well plates were transfected with 100 nM siRNA under normoxia using Lipofectamine RNAiMAX Reagent (Invitrogen) according to the manufacturer's instructions. Cells were used for experiments at 2 days after transfection. Then, cells were cultured additionally under normoxia and hypoxia in each experiment.

Plasmids

Plasmids pFN21A HaloTag CMV Flexi-RBPJ vector and pFN21AB5901 control empty vector were purchased from Promega (Madison, WI, USA). Cells (0.2×10^6 cells/well) seeded in 6-well plates were transfected with 2.5 μg plasmids under normoxia using Lipofectamine 3000 (Invitrogen) according to the manufacturer's instructions. Cells were used for experiments at 1 day after transfection.

Immunoblotting

Whole cell extraction was performed with M-PER Reagents (Pierce Biotechnology, Rockford, IL, USA) according to the manufacturer's instructions. Protein concentration was determined with Bio-Rad Protein Assay (Bio-Rad, Hercules, CA, USA), and protein samples (50 μg) were separated by electrophoresis on an SDS–polyacrylamide gel and transferred to Protran nitrocellulose membranes (Whatman GmbH, Dassel, Germany). Blots were then incubated with anti-SMO Ab (1:200, sc-13943, Santa Cruz Biotechnology, Santa Cruz, CA, USA), anti-GLI1 Ab (1:100, sc-20687, Santa Cruz Biotechnology), anti-MAML3 Ab (1:100, sc-82220, Santa Cruz Biotechnology), anti-RBPJ Ab (1:100, sc-8213, Santa Cruz Biotechnology), anti-MMP2 Ab (1:100, sc-10736, Santa Cruz Biotechnology) and anti-α-tubulin Ab (1:1000, Sigma Aldrich Co., St. Louis, MO, USA) overnight at 4 °C. Blots were then incubated with the appropriate horseradish peroxidase-linked secondary antibody (Amersham Biosciences, Piscataway, NJ, USA) at room temperature for 1 hour. Immunocomplexes were detected with ECL plus Western Blotting Detection System (Amersham Biosciences) and visualized with a Molecular Imager FX (Bio-Rad). We used α-tubulin a protein loading control.

In vivo *xenograft tumor model*

Six-week-old female BALB/c nude mice were obtained from Charles River Laboratories Japan (Kanagawa, Japan) and acclimatized for a week. All animal procedures were approved by the Animal Care and Use Committee at Kyushu University (A25-027-1). Cultured SUIT-2 cells transfected with *MAML3*-targeting siRNA, *RBPJ*-targeting siRNA and non-targeting control siRNA were subcutaneously implanted into bilateral flank regions (5.0×10^5 cells in 50 μl of RPMI) of the BALB/c nude mice ($n = 8$). The tumor size was determined twice a week and the tumor volume was calculated with the following formula: $A \times B^2 \times 0.5$, where B is the smaller of the two perpendicular diameters. The mice were euthanized when the tumor size had reached 2 cm in diameter or if the animals had become moribund during the observation period.

Fluorescence immunohistochemistry

Slides from patients with pancreatic cancer were deparaffinized with xylene and rehydrated with alcohol; antigen retrieval was achieved by microwaving in Target Retrieval Solution (pH 6.0, DAKO, Japan) for 10 minutes. The sections were rinsed with phosphate-buffered saline (PBS) and blocked using Blocking One Histo (Nacalai Tesque) for 10 minutes at room temperature. The sections were incubated with anti-Ki67 (BD Phamingen), anti-VEGF (sc-152, Santa Cruz), anti-SMO (sc-13943, Santa Cruz), anti-RBPJ (Santa Cruz) and anti-MAML3 (Santa Cruz) antibodies overnight at 4 °C. Primary antibodies were then visualized by incubating slides with Alexa Fluor 488 conjugated donkey anti-mouse (1:1000; Invitrogen), Alexa Fluor 594 conjugated goat anti-rabbit (1:1000; Invitrogen) and Alexa Fluor 488 conjugated donkey anti-goat (1:1000; Invitrogen) for 1 hour at 37 °C, respectively. After incubation with secondary antibodies, sections were rinsed with PBS three times. Slides were counterstained with 4′,6-diamidino-2-phenylindole (DAPI, Sigma Aldrich) and then mounted by VectaShield (Vector Laboratories, Burlingame, CA, USA). The samples were examined by fluorescence microscopy (Carl Zeiss, Tokyo, Japan). Informed consent was obtained from all individuals.

Statistical analysis

The data are presented as means ± standard deviation (SD). Student's *t*-tests were used to compare continuous variables between two groups. Chi-squared test was used to analyze the tumorigenicity in mice. All statistical analyses were performed using Microsoft Excel software (Microsoft Corp., Redmond, WA, USA). *P*-values of <0.05 were considered as statistically significant.

Results

Recombination signal binding protein for immunoglobulin-kappa-J region (RBPJ) contributes to hypoxia-induced upregulation of SMO transcription

To identify genes involved in the upregulation of SMO transcription under hypoxia, we compared one of PDAC lines, ASPC-1 cells cultured under hypoxia for 2 days with ASPC-1 cells cultured under normoxia and analyzed changes in expression of genes related to Hh signaling by DNA microarray analysis. Of the genes identified by GeneMANIA as exhibiting differential expression patterns, we found four candidate genes that showed a difference of expression of ≥2.0-fold (Supplementary Table S1). RBPJ, a transcriptional regulator, was among the identified genes and thus we selected it as a candidate for further investigation.

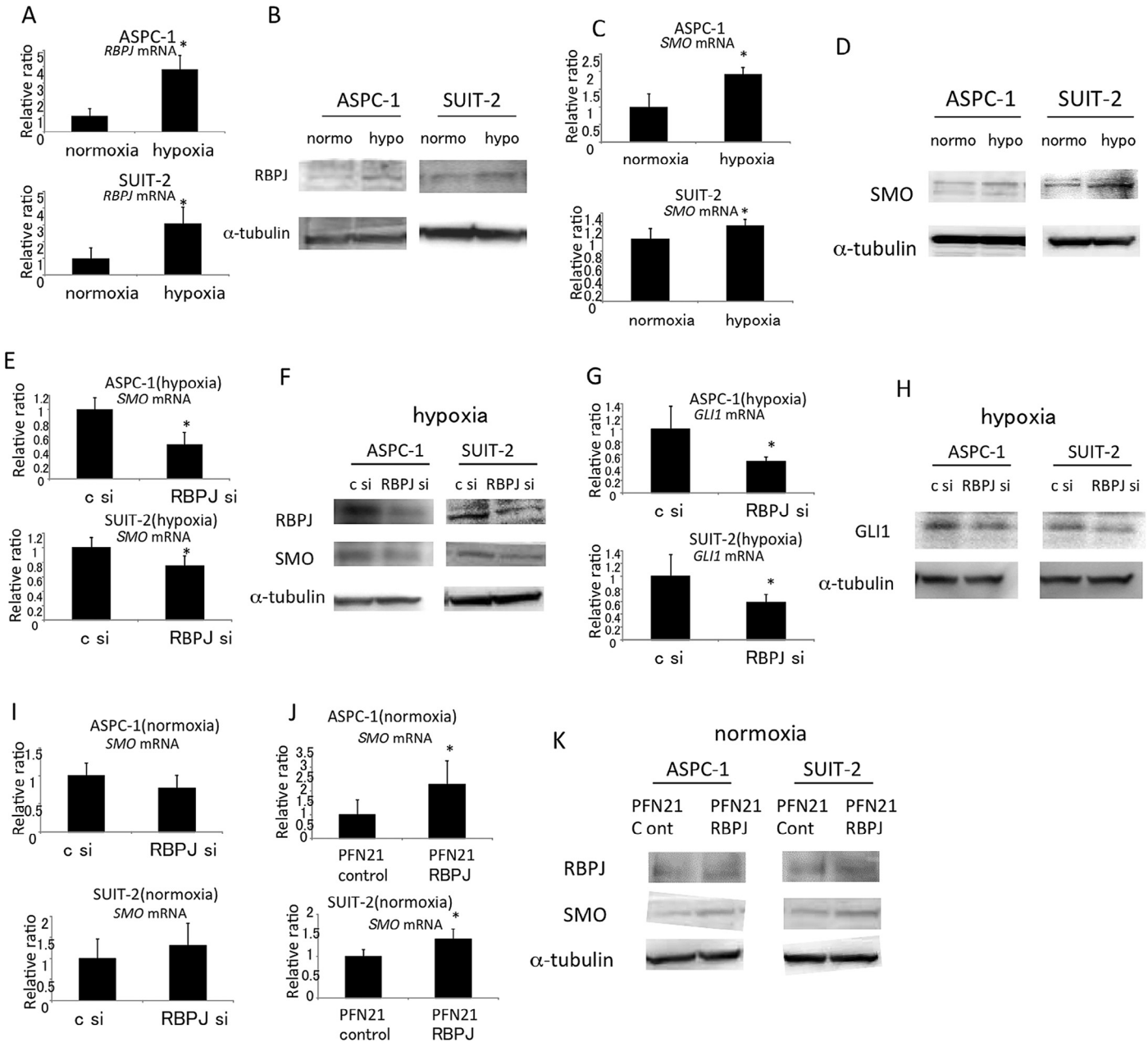

Fig. 1. RBPJ contributes to hypoxia-induced upregulation of *SMO* transcription. *RBPJ* mRNA (A) and protein (B) expressions were estimated in PDAC cultured for 24 h under hypoxic condition by real time RT-PCR and western blot, respectively. *SMO* mRNA (C) and protein (D) expressions were estimated in PDAC cultured for 24 h under hypoxic condition by real time RT-PCR and western blot, respectively. SMO mRNA (E), SMO protein (F), GLI1 mRNA (G), and GLI1 protein (H) expressions in RBPJ siRNA-transfected PDAC cultured under hypoxia for 24 h were investigated by real-time PCR and western blotting. (I) *SMO* mRNA expression in *RBPJ* siRNA-transfected PDAC cultured under hypoxia for 24 h were evaluated by real time RT-PCR. SMO mRNA (J) and protein (K) expressions in RBPJ plasmid-transfected PDAC cultured under normoxia were estimated by real time PCR and western blotting, respectively.

To confirm the microarray analysis, we examined RBPJ expression by real-time PCR and western blot. The results confirmed that RBPJ and SMO mRNA and protein expressions were increased under hypoxia compared to normoxia in both PDAC lines, ASPC-1 and SUIT-2 cells (Fig. 1A–D). To determine whether RBPJ contributes to hypoxia-induced upregulation of SMO transcription, we knocked down RBPJ expression using *RBPJ* siRNA. Importantly, SMO mRNA and protein expressions in *RBPJ* siRNA-transfected PDAC were significantly decreased under hypoxia compared to controls (Fig. 1E and F). In addition, the mRNA and protein levels of GLI1, a downstream factor of Hh signaling, were significantly decreased under hypoxia in *RBPJ* siRNA-transfected PDAC compared with controls (Fig. 1G and H). Interestingly, there was no significant difference in *SMO* mRNA expression between *RBPJ* siRNA-transfected PDAC and controls under normoxic condition (Fig. 1I). Conversely, when RBPJ was overexpressed by RBPJ plasmid transfection under normoxia, SMO mRNA and protein expressions were significantly increased (Fig. 1J and K). These results suggest that RBPJ may contribute to hypoxia-induced upregulation of SMO transcription.

RBPJ contributes to proliferation and invasiveness of PDAC under hypoxic condition

Next we investigated whether RBPJ affects cellular processes that are critical in inducing malignant potential in PDAC such as proliferation and invasiveness. Proliferation of *RBPJ* siRNA-transfected PDAC

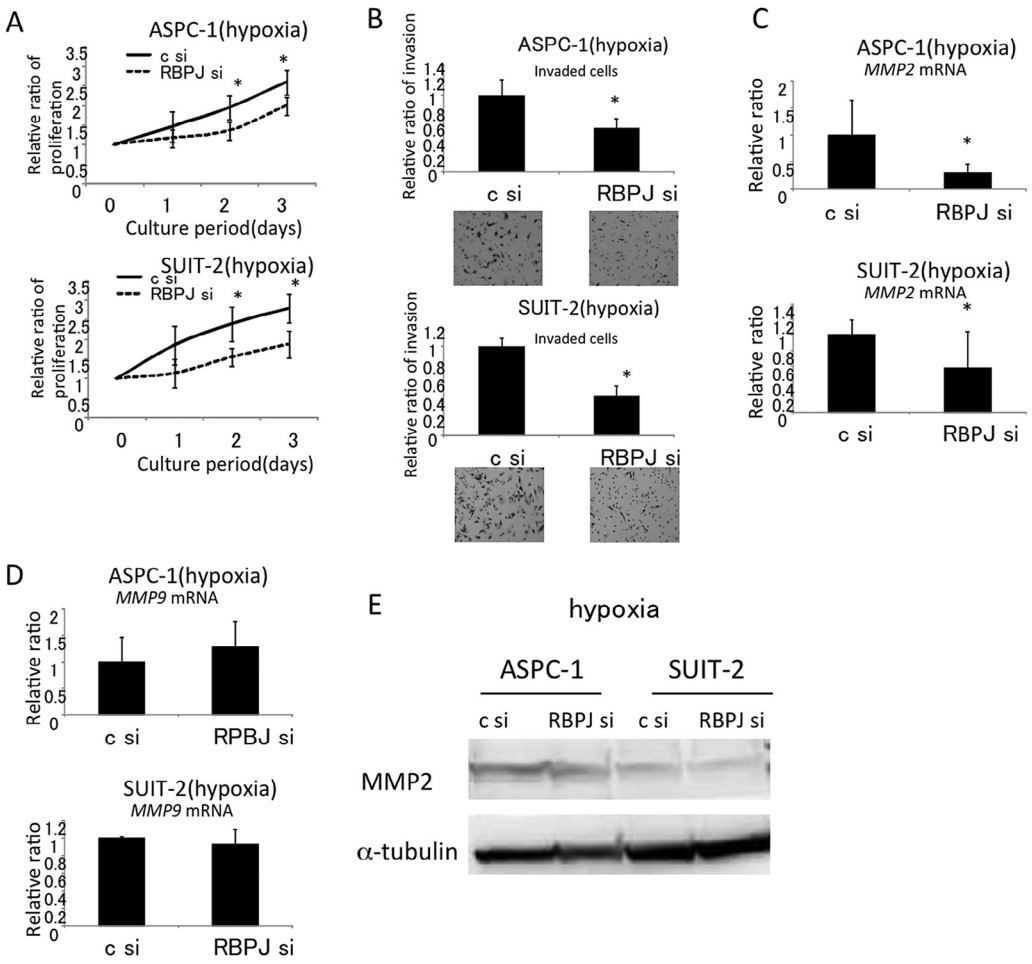

Fig. 2. RBPJ is involved with proliferation and invasiveness in PDAC under hypoxia. (A) *RBPJ* siRNA-transfected PDAC (1.0×10^5 cells/well) were plated to 6-well plates and cultured under hypoxia, and cell numbers were counted by light microscopy at the indicated days. (B) *RBPJ* siRNA-transfected PDAC (1.0×10^5 cells) were added to the upper side of the transmembrane. After incubation under hypoxia for 24 h, cells that migrated to the lower side of the transmembrane were stained by Giemsa and total cell numbers were counted. Representative photos were shown. Original magnification is 100×. *MMP-2* (C) and *MMP-9* (D) mRNA expressions in *RBPJ* siRNA-transfected PDAC cultured under hypoxia for 24 h were determined by real time RT-PCR. (E) MMP-2 protein expression was investigated by western blotting. $^*P < 0.05$; bar, SD.

was significantly inhibited under hypoxia compared with controls (Fig. 2A). Invasiveness of *RBPJ* siRNA-transfected PDAC was also significantly suppressed under hypoxia compared with controls (Fig. 2B). We have already demonstrated that both MMP-2 and MMP-9 contribute to the invasiveness in PDAC under hypoxia [13]. To examine the mechanisms underlying the effects of RBPJ on invasiveness, we analyzed MMP levels. In *RBPJ* siRNA-transfected PDAC cultured under hypoxia for 24 h, we found decreased expression of MMP-2 mRNA but not MMP-9 mRNA (Fig. 2C and D). MMP-2 protein expression in RBPJ siRNA-transfected PDAC was also decreased compared to controls (Fig. 2E). In addition, because we previously showed that Hh signaling activation contributes to induce malignant potential in PDAC under hypoxia [4,5,12,13], taken together, these results suggest that RBPJ contributes to proliferation and invasiveness in PDAC under hypoxic condition through Hh signaling activation.

Mastermind-like 3 (MAML3) contributes to hypoxia-induced upregulation of SMO transcription

RBPJ forms a complex with Notch intracellular domain (NICD) and the transcriptional co-activator, MAML3, in the nucleus to transcribe target genes. Thus, we next evaluated MAML3 expression to examine if MAML3 contributes to SMO upregulation under hypoxia. Interestingly, DNA microarray analysis showed that MAML3 expression was also increased under hypoxia (ratio of MAML3 expression under hypoxia to under normoxia: 1.44). We confirmed that MAML3 mRNA and protein expressions under hypoxia were increased compared with those under normoxia by real time PCR and western blot analysis (Fig. 3A and B). Importantly, SMO and GLI1 mRNA and protein expressions in *MAML3* siRNA-transfected PDAC were significantly decreased compared with controls (Fig. 3C–E). Interestingly, there was no significant difference in *SMO* mRNA expression between *MAML3* siRNA-transfected PDAC and controls under normoxic condition (Fig. 3F). These results suggest that MAML3 is involved with increased SMO transcription under hypoxia in PDAC.

MAML3 contributes to proliferation and invasiveness in PDAC under hypoxic condition

Next we examined whether MAML3 affected the induction of malignant phenotype in PDAC under hypoxia. Proliferation was significantly suppressed by MAML3 inhibition in PDAC under hypoxic condition (Fig. 4A). Invasiveness in *MAML3* siRNA-transfected PDAC was significantly lower than that in control under hypoxia (Fig. 4B). In *MAML3* siRNA-transfected PDAC cultured under hypoxia, we found decreased expression of MMP-2 mRNA but not MMP-9 mRNA (Fig. 4C and D). MMP-2 protein expression in *MAML3* siRNA-transfected PDAC

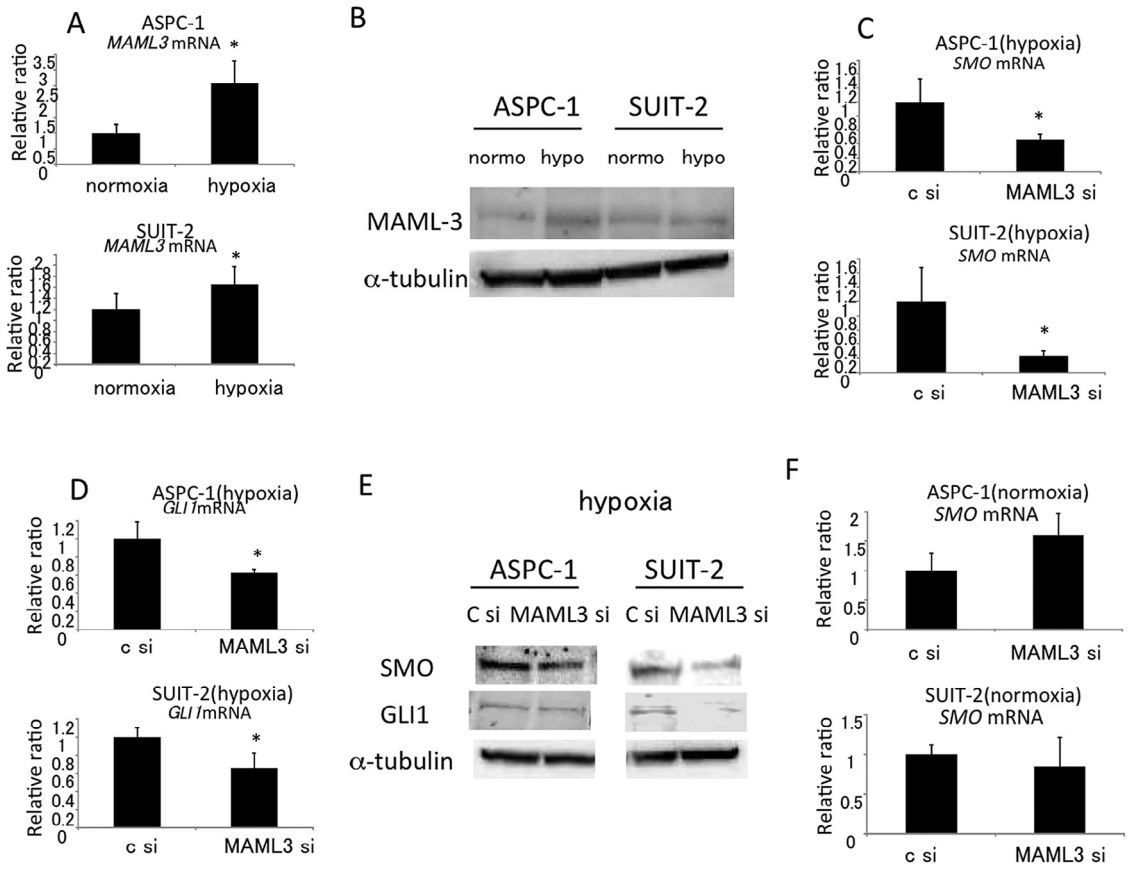

Fig. 3. Hh signaling is activated through upregulation of MAML3 under hypoxia. *MAML3* mRNA (A) and protein (B) expressions in PDAC cultured for 24 h under hypoxic conditions were estimated by real time RT-PCR and western blot. *SMO* (C) and *GLI1* (D) mRNA expressions in MAML3 siRNA-transfected PDAC cultured under hypoxia for 24 h were evaluated by real-time RT-PCR. (E) SMO and GLI1 protein expressions in MAML3 siRNA-transfected PDAC cultured under hypoxia for 24 h were analyzed by western blotting. (F) *SMO* mRNA expression in *MAML3* siRNA-transfected PDAC cultured under normoxic condition was evaluated by real time RT-PCR. $^{*}P < 0.05$; bar, SD.

was also decreased compared with controls (Fig. 4E). These results suggest that MAML3 contributes to proliferation and invasiveness in PDAC under hypoxic condition through Hh signaling activation.

RBPJ and MAML3 are involved with proliferation and tumorigenesis in vivo

To evaluate the effect of RBPJ and MAML3 on proliferation and tumorigenesis *in vivo*, mice were implanted with SUIT-2 cells transfected with *RBPJ*-targeting siRNA, *MAML3*-targeting siRNA or non-targeting control siRNA were subcutaneously implanted into the bilateral flank regions in BALB/c nude mice (n = 8). Tumorigenesis and tumor volume in mice implanted with *RBPJ*-inhibited and *MAML3*-inhibited SUIT-2 cells were significantly lower than those in control mice (Table 1 and Fig. 5A). Next, to analyze this mechanism for decreased growth, we performed Ki67 and VEGF staining on tumors from mice, which showed that tumors from mice injected with SUIT-2 cells transfected with *RBPJ*-siRNA and *MAML3*-siRNA have lower Ki67 and VEGF expressions than tumors from cells transfected with *control* siRNA (Fig. 5B and C). These results suggest that decreased proliferation and angiogenesis involved decreased tumor volume. Furthermore, consistently, immunofluorescence staining of pancreatic cancer in surgically resected specimens demonstrated that RBPJ and MAML3 were co-expressed with SMO in all 10 specimens (Fig. 5D).

Discussion

In the present study, we demonstrated two novel findings. One is that expression of MAML3 and RBPJ increases under hypoxia but not normoxia conditions. Second, we show that these augmentations contribute to the increase of SMO transcription under hypoxia, but not normoxia, to induce malignant phenotypes in PDAC.

Notch signaling and Hh signaling are both morphogenesis signaling pathways, and the re-activation of Notch signaling in cancer has been the subject of attention. RBPJ forms a complex with the NICD that is stabilized by MAML3, and Notch signaling is activated by binding of the RBPJ/NICD/MAML3 complex to DNA in the nucleus [14]. Indeed, the expression of Hes1-3 that is a Notch signaling target gene was suppressed by RBPJ and MAML3 inhibition (Supplementary Fig. S1), suggesting that RBPJ and MAML3 were involved with Notch signaling activation. A previous report showed that Notch ligand and NICD increased under hypoxic condition, and Notch signaling was subsequently activated [15]. Moreover, RBPJ and MAML3 have been suggested to interact with Hh signaling in this study. Thus, it is likely that the RBPJ/MAML3/NICD complex regulates SMO transcription under hypoxia. However, whether the RBPJ/MAML3/NICD complex regulates SMO expression directly or indirectly, and which NICD type, among Notch 1, Notch 2, Notch 3 and Notch 4, are involved in increased SMO expression under hypoxia are unclear (Supplementary Fig. S2). The research toward upregulation of RBPJ and MAML3 under hypoxia will lead to the explication of crosstalk between Hh signaling and Notch signaling for cancer treatment.

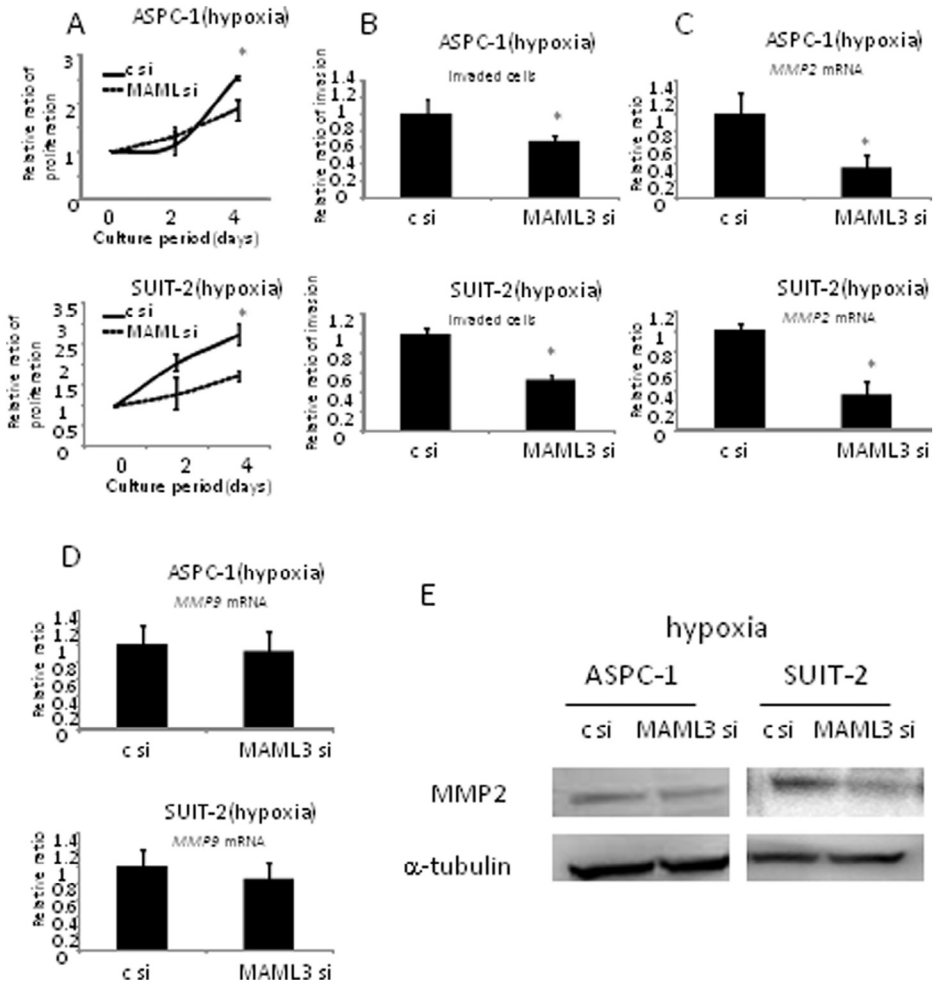

Fig. 4. MAML3 contributes to proliferation and invasiveness in PDAC under hypoxia. (A) *MAML3* siRNA-transfected PDAC (1.0×10^5 cells/well) were plated to 6-well plate and cultured under hypoxia, and cell number was counted by light microscopy at the indicated days. (B) *MAML3* siRNA-transfected PDAC (1.0×10^5 cells) were added to the upper chamber. After incubation under hypoxia for 24 h, cells that migrated to the lower chamber were stained by Giemsa and total cell number was counted. *MMP-2* (C) and *MMP-9* (D) mRNA expressions in MAML3 siRNA-transfected PDAC cultured under hypoxia for 24 h were determined by real time RT-PCR. (E) MMP-2 protein expression was investigated by western blotting. $^*P < 0.05$; bar, SD.

The mechanism of augmented RBPJ or MAML3 expressions under hypoxia also remains unclear. The results that regulation of SMO transcription by RBPJ or MAML3 may be limited under hypoxic condition are novel and interesting. Unlike during hypoxia, RBPJ and MAML3 expressions are considerably low under normoxia and therefore RBPJ and MAML3 may not contribute much to SMO transcription under normoxia. Although VEGF that is a target gene of a representative transcriptional factor under hypoxia, hypoxia inducible factor-1α (HIF-1α), may contribute significantly in tumor proliferation in mice (Fig. 5C), HIF-1α did not play a role for the expressions of *SMO* [4], *GLI1* [4], *MAML3* and *RBPJ* mRNAs (Supplementary Fig. S3). We anticipate that clarifying the interaction or crosstalk between Notch signaling and Hh signaling related to RBPJ and MAML3 under hypoxia may lead to the development of a new effective molecular targeted therapy for pancreatic cancer.

Degradation of type IV collagen in the basement membrane is required for cell invasion into adjacent blood or lymphatic vessels. MMPs play pivotal roles in the degradation of the extracellular matrix [16]. MMP-2 and MMP-9 are type IV collagenases that degrade type IV collagen [17]. Previously we showed that both MMP-2 and MMP-9 contributed to hypoxia-induced PDAC invasiveness [4,12]. However, in the present study, MMP-2, but not MMP-9, was involved in the invasiveness induced by RBPJ and MAML3 (Figs. 2 and 3). This suggests that various signaling pathways may contribute to the increased invasiveness under hypoxia.

It is difficult for *in vivo* mouse model to perform the experiment under hypoxic condition along with *in vitro* experiment. In the present study, cancer cells were administrated subcutaneously into mice. Subcutaneous O_2 was reported to be about 8% [18], which is hypoxic compared with the *in vitro* culture condition of 20% O_2. Therefore, our *in vivo* experiment under hypoxia was thought to be granted. The

Table 1
Tumorigenesis in mice implanted with SUIT2 cells transfected with control, *MAML3* or *RBPJ* siRNA.

Week	c-si (n = 8)	*MAML3*-si (n = 8)	*RBPJ*-si (n = 8)
1	6	[a]2*	3
1.5	7	[a]3*	[b]3*
2	8	[a]4*	[b]4*
2.5	8	5	[b]4*

[a] Comparison of the number of mice that formed tumor between control siRNA transfected SUIT-2 cell-injected mice vs. *MAML3* siRNA transfected SUIT-2 cell-injected mice.
[b] Comparison of the number of mice that formed tumor between control siRNA transfected SUIT-2 cell-injected mice vs. *RBPJ* siRNA transfected SUIT-2 cell-injected mice.
* $P < 0.05$ calculated by chi-squared test.

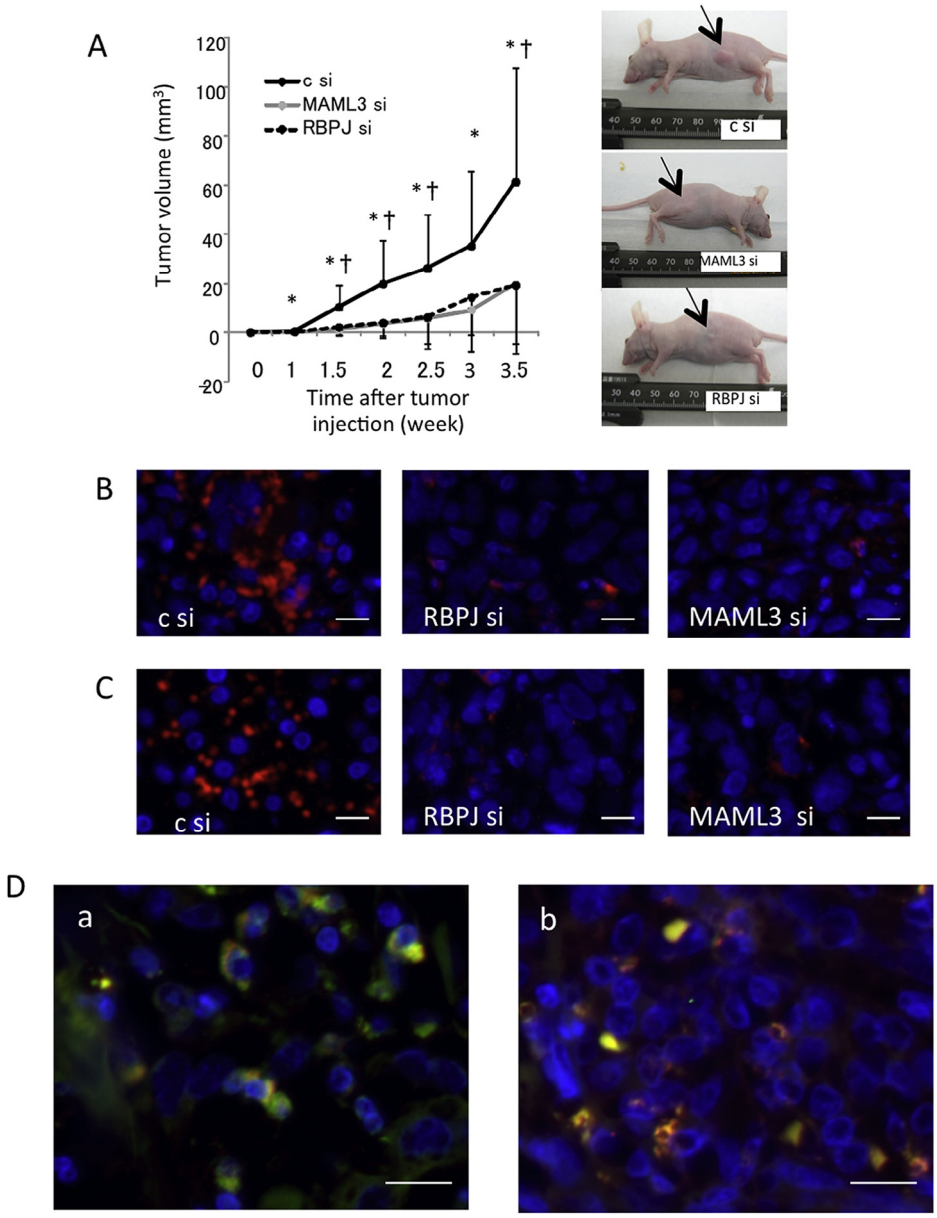

Fig. 5. RBPJ and MAML3 contribute to tumor proliferation in vivo. (A) SUIT-2 cells transfected with *MAML3*-targeting siRNA, *RBPJ*-targeting siRNA or non-targeting control siRNA were subcutaneously implanted into the bilateral flank regions (5.0×10^5 cells in 50 μl of RPMI) of BALB/c nude mice (n = 8). The tumor size was determined on the indicated days. Representative photos of mice (3.5 weeks after tumor injection) were shown. Arrow shows tumors. (B, C) Ki67 (B) and VEGF (C) immunofluorescence (IF) stainings were performed using tumors from mice. Original magnification is 400×. (D) Representative pictures of IF staining of surgically resected pancreatic cancer specimens for RBPJ (green; Alexa488) and SMO (red; Alexa594) (D-a), or MAML3 (green; Alexa488) and SMO (red; Alexa594) (D-b). Original magnification is 400×. *Comparison of tumor size between control vs. *MAML3* siRNA group. †Comparison of tumor size between control vs. *RBPJ* siRNA group. $P < 0.05$; bar, SD. Scale bar; 50 μm.

kinetics of tumor volume and tumorigenesis growth with RBPJ inhibition and MAML3 inhibition were similar (Table 1 and Fig. 5A), suggesting that the RBPJ/MAML3/NICD complex in the nucleus plays a pivotal role in tumor proliferation and tumorigenesis.

We also identified increased expressions of RBPJ and MAML3 mRNA in chronic hypoxia resistant ASPC-1 cells [19] as a stable hypoxic cell by DNA microarray analysis. RBPJ and MAML3 expressions in chronic hypoxia resistant ASPC-1 cells were increased by 1.42- and 2.22-fold, respectively, compared with those in ASPC-1 cells cultured under normoxia (Supplementary Table S2). This result supports our findings in the present study.

Previously, we have shown that GLI1 expression in SMO siRNA transfected PDAC was significantly lower than that in control siRNA transfected PDAC under hypoxia [4]. We have also revealed that MMP2 expression in GLI1-siRNA transfected PDAC was significantly lower than that in control siRNA transfected PDAC under hypoxia [13]. Our revised proposed model based on our findings is shown in Fig. 6. RBPJ and MAML3 positively regulate SMO transcription in PDAC under hypoxia. Our results suggest that RBPJ and MAML3 may be key players for the regulation of hypoxia-induced augmentation of SMO transcription and that RBPJ and MAML3 could be therapeutic targets for pancreatic cancer. While our results from the *in vitro* experiments are promising, the clinical trials using Hh inhibitors against pancreatic cancer have not been successful, suggesting that the hypoxic environment that upregulates SMO transcription must be taken into consideration. Our findings may lead to the development of the new effective therapeutic strategy for refractory pancreatic cancer.

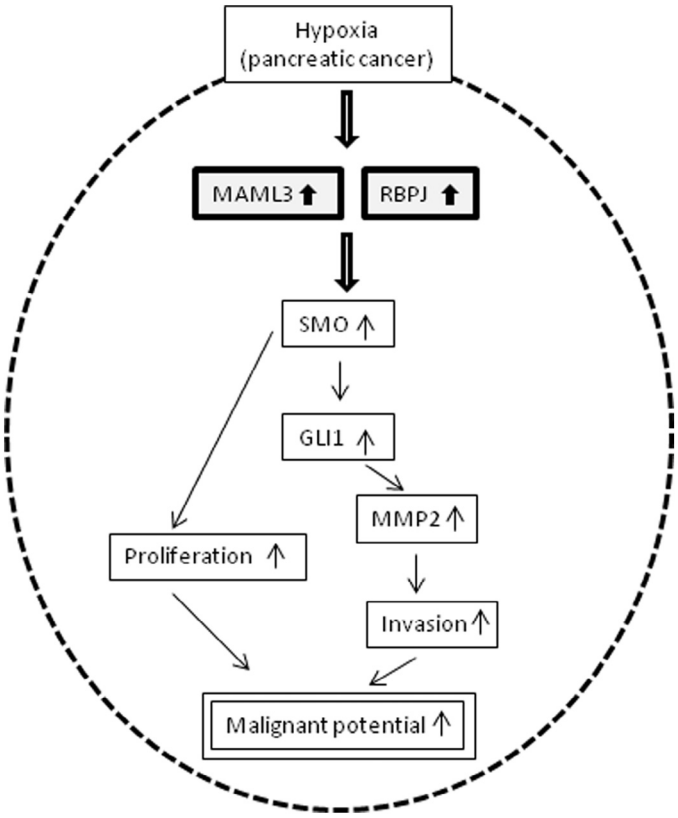

Fig. 6. Model of our findings in this study. MAML3 and RBPJ expressions increase under hypoxia. Then, MAML3 and RBPJ may positively regulate SMO transcription under hypoxia to induce malignant phenotype such as proliferation and invasiveness in PDAC. Bold lines showed new findings in this study.

Funding

This study was supported by the Japan Society for the Promotion of Science KAKENHI Grant Number 26293289.

Acknowledgments

We thank Ms. Kaori Nomiyama for skillful technical assistance.

Conflict of interest

The authors declare no conflict of interest for this work.

Appendix: Supplementary material

Supplementary data to this article can be found online at doi:10.1016/j.canlet.2015.11.012.

References

[1] A.C. Koong, V.K. Mehta, Q.T. Le, G.A. Fisher, D.J. Terris, J.M. Brown, et al., Pancreatic tumors show levels of hypoxia, Int. J. Radiat. Oncol. Biol. Phys. 48 (2000) 919–922.
[2] C.C. Caldwell, H. Kojima, D. Lukashev, J. Armstrong, M. Farber, S.G. Apasov, et al., Differential effects of physiologically relevant hypoxic conditions on T lymphocyte development and effector functions, J. Immunol. 167 (2001) 6140–6149.
[3] S. Hockel, K. Schlenger, P. Vaupel, M. Hockel, Association between host tissue vascularity and the prognostically relevant tumor vascularity in human cervical cancer, Int. J. Oncol. 19 (2001) 827–832.
[4] H. Onishi, M. Kai, S. Odate, H. Iwasaki, Y. Morifuji, T. Ogino, et al., Hypoxia activates the hedgehog signaling pathway in a ligand-independent manner by upregulation of SMO transcription in pancreatic cancer, Cancer Sci. 102 (2011) 1144–1150.
[5] H. Onishi, Y. Morifuji, M. Kai, K. Suyama, H. Iwasaki, M. Katano, Hedgehog inhibitor decreases chemosensitivity to 5-fluorouracil and gemcitabine under hypoxic conditions in pancreatic cancer, Cancer Sci. 103 (2012) 1272–1279.
[6] J. Lei, J. Ma, Q. Ma, X. Li, H. Liu, Q. Xu, et al., Hedgehog signaling regulates hypoxia induced epithelial to mesenchymal transition and invasion in pancreatic cancer cells via a ligand-independent manner, Mol. Cancer 12 (2013) 66.
[7] T.R. Spivak-Kroizman, G. Hostetter, R. Posner, M. Aziz, C. Hu, M.J. Demeure, et al., Hypoxia triggers hedgehog-mediated tumor-stromal interactions in pancreatic cancer, Cancer Res. 73 (2013) 3235–3247.
[8] A. Sekulic, M.R. Migden, A.E. Oro, L. Dirix, K.D. Lewis, J.D. Hainsworth, et al., Efficacy and safety of vismodegib in advanced basal-cell carcinoma, N. Engl. J. Med. 366 (2012) 2171–2179.
[9] F.C. Kelleher, Hedgehog signaling and therapeutics in pancreatic cancer, Carcinogenesis 32 (2011) 445–451.
[10] S. Sandhiya, G. Melvin, The dawn of hedgehog inhibitors: vismodegib. J. Pharmacol. Pharmacother. 4 (2013) 4–7.
[11] S.X. Atwood, A.L. Chang, A.E. Oro, Hedgehog pathway inhibition and the race against tumor evolution, J. Cell Biol. 199 (2012) 193–197.
[12] H. Onishi, M. Katano, Hedgehog signaling pathway as a new therapeutic target in pancreatic cancer, World J. Gastroenterol. 20 (2014) 2335–2342.
[13] H. Onishi, T. Morisaki, F. Nakao, S. Odate, T. Morisaki, M. Katano, Protein-bound polysaccharide decreases invasiveness and proliferation in pancreatic cancer by inhibition of hedgehog signaling and HIF-1α pathways under hypoxia, Cancer Lett. 335 (2013) 289–298.
[14] J.L. Ables, J.J. Breunig, A.J. Eisch, P. Rakic, Not(ch) just development: notch signalling in the adult brain, Nat. Rev. Neurosci. 12 (2011) 269–283.
[15] L. Marignol, K. Rivera-Figueroa, T. Lynch, D. Hollywood, Hypoxia, notch signalling, and prostate cancer, Nat. Rev. Urol. 10 (2013) 405–413.
[16] A.A. Kamat, M. Fletcher, L.M. Gruman, P. Mueller, A. Lopez, C.N. Landen Jr., et al., The clinical relevance of stromal matrix metalloproteinase expression in ovarian cancer, Clin. Cancer Res. 12 (2006) 1707–1714.
[17] A.R. Nelson, B. Fingleton, M.L. Rothenberg, L.M. Matrisian, Matrix metalloproteinases: biologic activity and clinical implications, J. Clin. Oncol. 18 (2000) 1135–1149.
[18] A. Carreau, B. El Hafny-Rahbi, A. Matejuk, C. Grillon, C. Kieda, Why is the partial oxygen pressure of human tissues a crucial parameter? Small molecules and hypoxia, J. Cell. Mol. Med. 15 (2011) 1239–1253.
[19] Y. Morifuji, H. Onishi, H. Iwasaki, A. Imaizumi, K. Nakano, M. Tanaka, et al., Reoxygenation from chronic hypoxia promotes metastatic processes in pancreatic cancer through the Hedgehog signaling, Cancer Sci. 105 (2014) 324–333.